We are IntechOpen, the world's leading publisher of Open Access books Built by scientists, for scientists

4,800
Open access books available

122,000
International authors and editors

135M
Downloads

Our authors are among the

154
Countries delivered to

TOP 1%
most cited scientists

12.2%
Contributors from top 500 universities

CLARIVATE ANALYTICS BOOK CITATION INDEX INDEXED

WEB OF SCIENCE™

Selection of our books indexed in the Book Citation Index in Web of Science™ Core Collection (BKCI)

Interested in publishing with us?
Contact book.department@intechopen.com

Numbers displayed above are based on latest data collected.
For more information visit www.intechopen.com

Chapter 6

Dynamic Amplification of Optical Signals by Photorefractive Ferroelectric Liquid Crystals

Takeo Sasaki

Additional information is available at the end of the chapter

http://dx.doi.org/10.5772/60776

Abstract

In this chapter, the photorefractive effect in photoconductive ferroelectric liquid crystal blends is described. A blend of liquid crystals that form chiral smectic C phase and photoconductive compounds shows the photorefractive effect. The ferroelectric liquid crystal blends containing a photoconductive chiral compound were found to exhibit a gain coefficient of over 1200 cm^{-1} and the response time of sub-millisecond. Using the blend, real-time dynamic amplification of an optical image signal of over 30 fps was demonstrated.

Keywords: Ferroelectric liquid crystals, photorefractive effect, semiconductor, photoconductivity, hologram

1. Introduction

Ferroelectric liquid crystals (FLCs) have attracted significant interest from both fundamental and practical perspectives [1, 2]. Even though liquid crystals (LCs) are liquid, some of them exhibit ferroelectricity. The response of FLCs to an applied electric field is very fast, in the range of a few tens of microseconds to a few milliseconds. The fast response of FLCs is advantageous for display applications; however, the treatment of FLCs requires sophisticated techniques because FLCs are very viscous. Displays that employ FLCs are not commercially available nowadays, due to the difficulty of fabrication into wide area displays. Recently, the photorefractive effect in FLCs was investigated, and FLCs were found to exhibit very high performance. The photorefractive effect is a phenomenon in which a dynamic hologram is

formed in a material. When two laser beams interfere in a photorefractive material, a refractive index grating is formed. This phenomenon is applicable to devices related to diffraction optics, including 3D displays, optical amplification, optical tomography, novelty filters, and phase-conjugate wave generators [3]. The unique feature of the photorefractive effect is the asymmetric energy exchange in two-beam coupling; when two laser beams interfere in a photorefractive material, the energy of one of the interfering beams is transferred to the other beam. The asymmetric energy exchange can be used to coherently amplify signal beams [4]; therefore, it has the potential to be used as a transistor for electrical circuits in a wide range of optical technologies (Figure 1). Optically transparent materials that possess both photovoltaic and electro-optic properties also exhibit the photorefractive effect. There have been a lot of studies to develop photorefractive materials, such as inorganic photoconductive ferroelectric crystals, organic photoconductive ferroelectric crystals, organic photoconductive polymers, amorphous organic photoconductive materials, photoconductive amphiphilic compounds, and photoconductive LCs [5-8]. Since 1991, organic materials have attracted significant interest because they exhibit large photorefractivity and a shorter response time compared with that of inorganic crystals [3, 7, 8]. The photorefractive effect induces a change in the refractive index by a mechanism that involves both photovoltaic and electro-optic effects (Figure 2). An organic photorefractive material is composed of a photoconductive compound, an electro-optic compound, and an electron-trap reagent. Thus, the active wavelength can be determined by the selection of the photoconductive compound. With interfering two laser beams in an organic photorefractive material, charge generation occurs at the bright positions of the interference fringe and the generated charges diffuse within the material. The distances of the diffusions of positive and negative charges are different in an organic material because the mobilities of the positive and negative charges are different. That leads to a formation of charge-separated state. The higher mobility charge diffuses over a longer distance than the lower mobility charge. While the charges with low mobility stay in the bright areas, the charges with high mobility diffuse to the dark areas. Thus, the bright area and dark area are charged with opposite polarities, and an internal electric field (space charge field) is formed in the area between the brightest and the darkest positions. The refractive indices of the areas are changed by the electro-optic effect. In such a way, a refractive index grating is produced. A high electric field of 10–50 V/μm is typically applied to a polymer film, aside from the internal electric field, to obtain photorefractivity. The polymer material is typically 100 μm thick, so that a voltage of 1–5 kV is required to apply on the film to achieve photorefractivity, which is almost comparable to the breakdown voltage of the polymer film. This electric field is necessary for increasing the charge generation efficiency.

It is expected that a multiplex hologram display devices can be developed using photorefractive polymers [9, 10]. It was shown that clear 3D images were recorded in the photorefractive polymer film. However, if polymer photorefractive materials are put into practical uses, a high voltage (3–5 kV) required to activate the photorefractive effect in polymer materials must be improved. There have been reports on the photorefractive effect of LCs [11]. LCs can easily be driven by a low electric field because LCs are liquid in nature. The most well-known LC phases are nematic and smectic phases (Figure 3). LCs that show nematic phase are used in liquid crystal displays (LCDs). However, LCs that show smectic phases are very viscous so that they are seldom utilized in practical applications. The LCs of which the photorefractivity was firstly investigated were nematic LCs [11]. It was found that a large photorefractivity was obtained

http://dx.doi.org/10.5772/60776

with the application of low activation voltage (a few volts). The photorefractivity of ferroelectric liquid crystals doped with photoconductive compounds has been reported [12-14]. FLCs are considered to be candidates for practical photorefractive materials. A sub-millisecond refractive index grating formation time and a large gain coefficient are easily obtained in photorefractive FLCs.

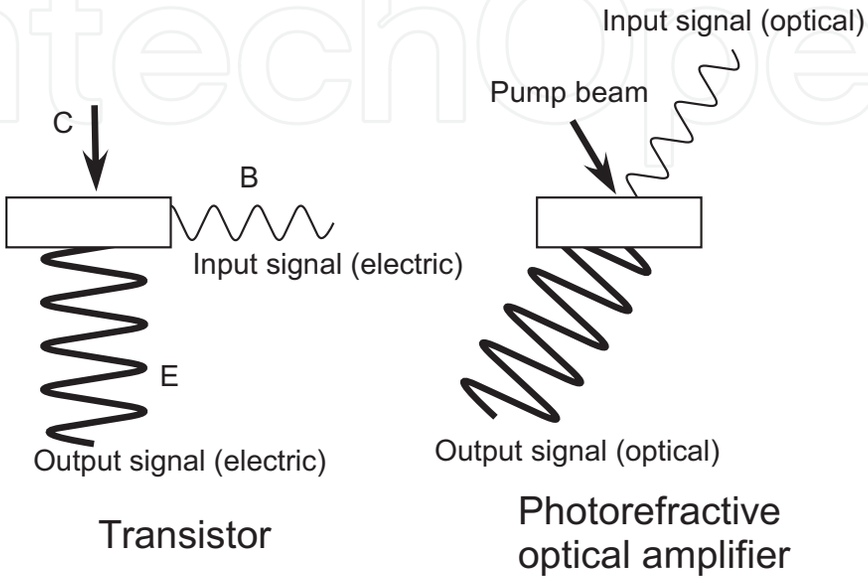

Figure 1. Transistor in electric circuit and photorefractive amplifier.

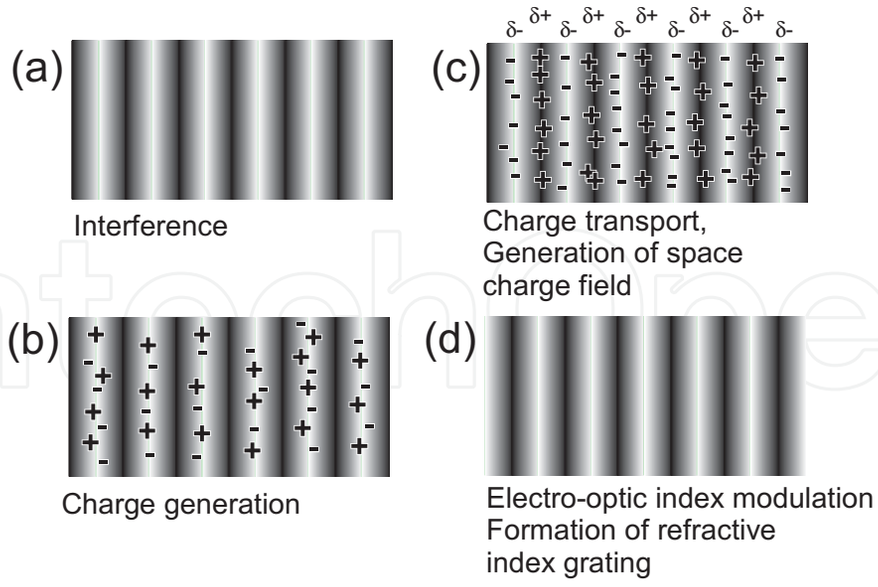

Figure 2. Schematic illustration of the mechanism for the photorefractive effect. (a) Two laser beams interfere in the photorefractive material; (b) charge generation occurs at the light areas of the interference fringes; (c) electrons are trapped at the trap sites in the light areas, holes migrate by diffusion or drift in the presence of an external electric field, and generate an internal electric field between the light and dark positions; (d) the refractive index of the corresponding area is altered by the internal electric field that is generated.

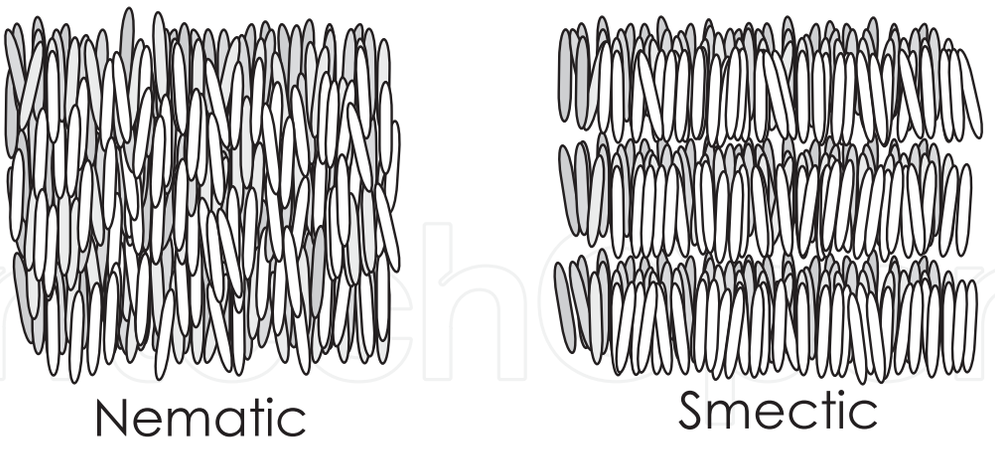

Figure 3. Structures of the nematic and smectic phases.

2. Ferroelectric liquid crystals

In 1974, Meyer suggested theoretically that LCs that form an LC phase with low symmetry should exhibit ferroelectricity [15]. Meyer instructed the synthesis of a liquid crystalline molecule that exhibits the smectic C (SmC) phase and also possesses chiral structure and permanent dipole moment. The structure of the LC molecule (DOBANBC) is shown in Figure 4. As Meyer had expected, DOBANBC was found to exhibit ferroelectricity. After the discovery of ferroelectricity in LCs, an intensive search for FLCs was conducted by many researchers, including LCD developers. As a result, it was determined that not only pure liquid crystalline compounds, but also mixtures of smectic LC compounds and chiral compounds exhibit ferroelectric phases. This was very advantageous for practical applications because clear, defect-free large-area panels could be realized using such mixtures and the properties of the mixtures could be adjusted by the selection of appropriate component compounds. In 1997, a fast FLC display panel was commercially released by Canon.

FLCs belong to the class of smectic LCs that have a layered structure [1, 2, 15]. A typical FLC molecule consists of a central core, a carbonyl group, and a chiral unit (Figure 4). The dipole moment of an FLC molecule is perpendicular to the long molecular axis. FLCs exhibit a chiral smectic C phase (SmC*) that possesses a helical structure. It should be noted here that to observe ferroelectricity in these materials, the FLCs must be formed into thin films [1] with a thickness of a few micrometers. When an FLC is sandwiched between glass plates to form a film with a thickness of a few micrometers, the helical structure of the SmC* phase uncoils and a surface-stabilized state (SS-state) is formed in which ferroelectricity appears (Figure 5). The thickness of the FLC film is typically 2 μm when it is used in display applications. The FLC molecules are restricted to only two directions in such thin films. The state is termed as SS-state. The direction of the alignment of FLC molecules is changed by the change in direction of the spontaneous polarization (Figure 6). When an alternating electric field is applied to the SS-FLC, the FLC molecules perform a continuous switching motion. The response time of the

http://dx.doi.org/10.5772/60776

electrical switching in the FLCs is typically shorter than 1 ms. The direction of spontaneous polarization is governed by the applied electric field, which causes a change in the properties according to the direction of polarization. The mechanism for the photorefractive effect in FLCs is shown in Figure 7. When laser beams interfere in a mixture of an FLC and a photoconductive compound, internal electric fields are produced between the bright and dark positions of the interference fringe. The direction of spontaneous polarization in the area between the bright and dark positions of the interference fringes is changed by the internal electric field and a striped pattern of the FLC molecule orientations is induced. The process is different from those occur in other organic photorefractive materials. In a photorefractive FLC, the bulk polarization responds to the internal electric field. That is the base of the fast switching of FLC molecules.

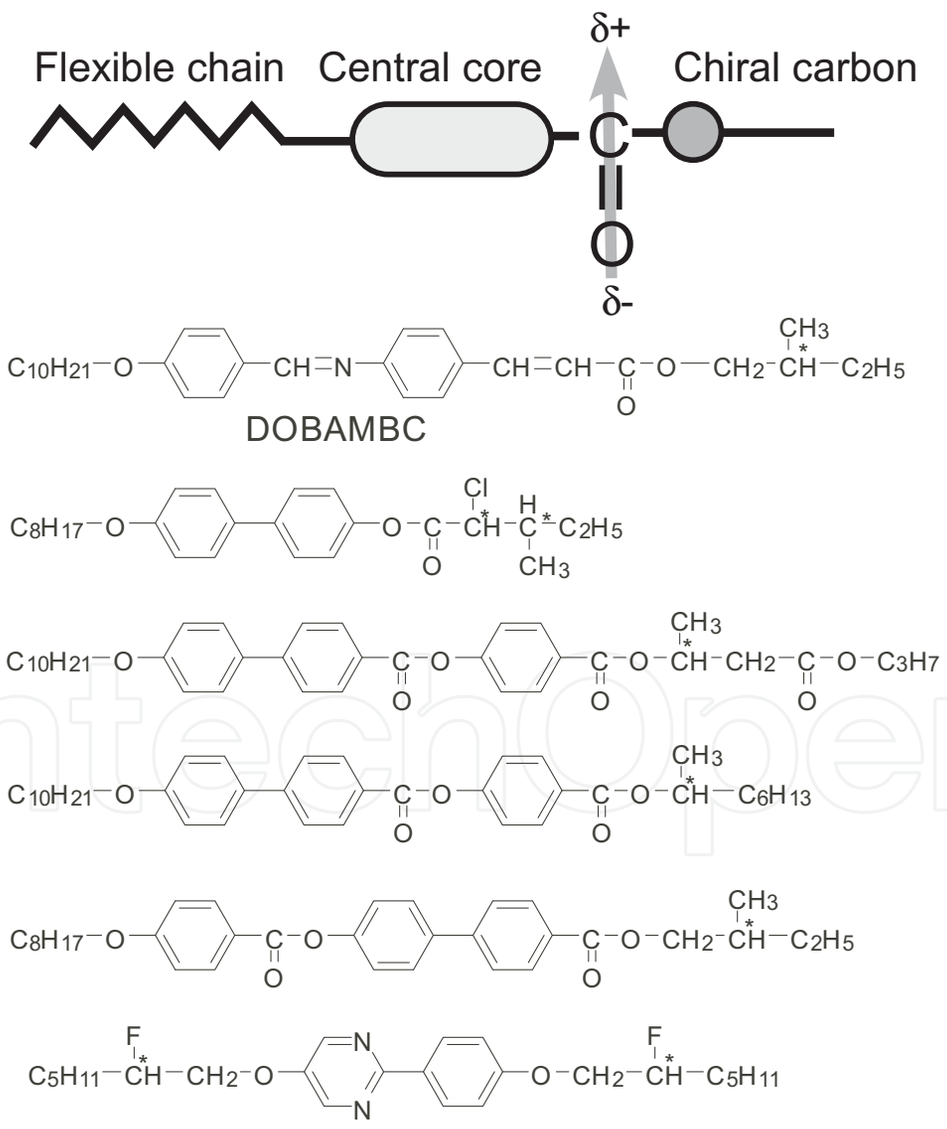

Figure 4. Molecular structures of FLCs.

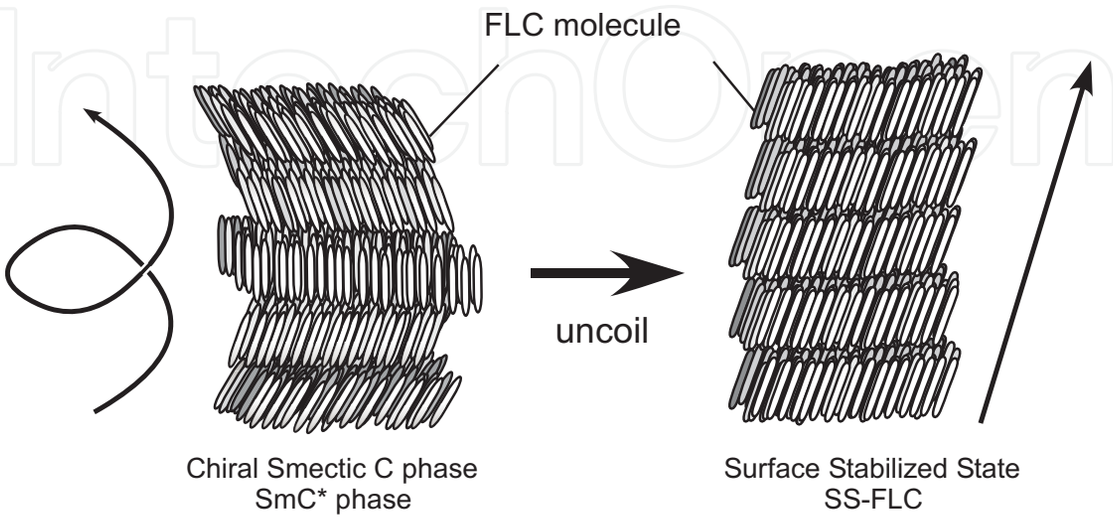

Figure 5. Structures of the SmC phase and the SS-state of the SmC phase (SS-FLC).

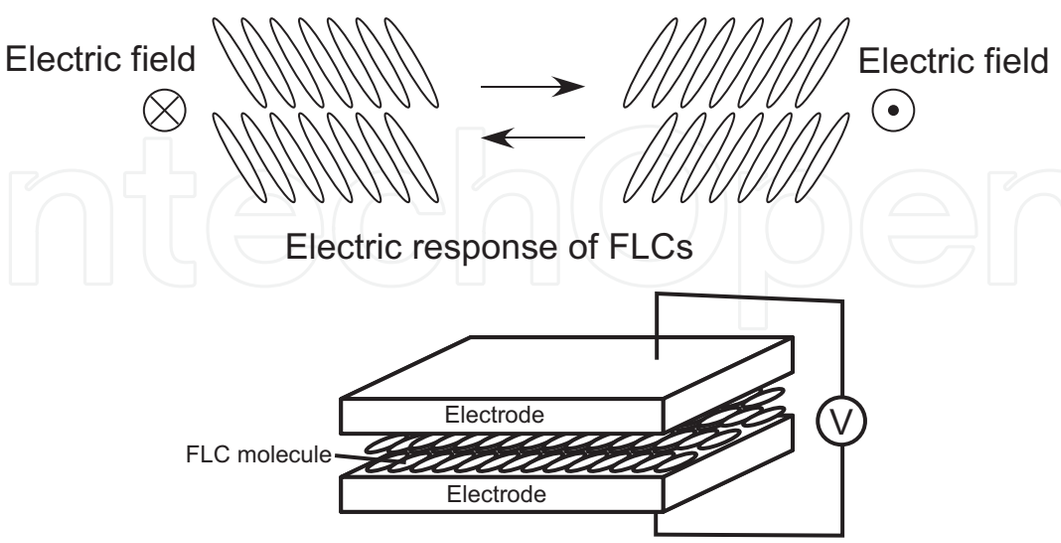

Figure 6. Electro-optical switching in the SS-state of FLCs.

http://dx.doi.org/10.5772/60776

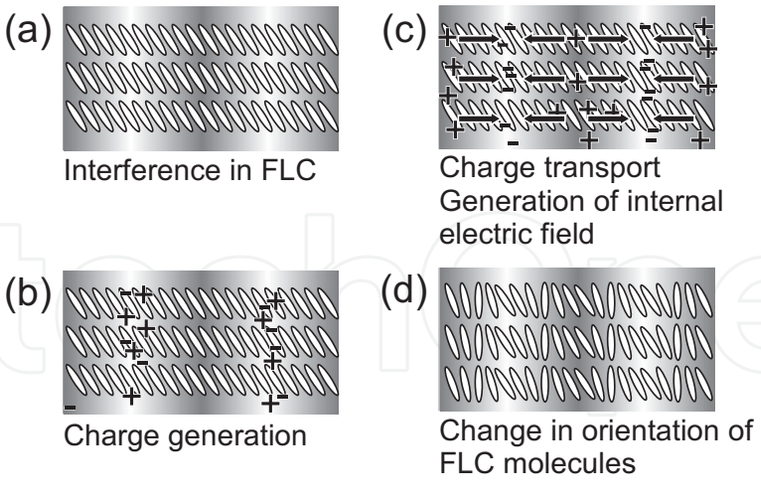

Figure 7. Schematic illustration of the mechanism for the photorefractive effect in FLCs. (a) Two laser beams interfere in the SS-state of the FLC/photoconductive compound mixture; (b) charge generation occurs at the light areas of the interference fringes; (c) electrons are trapped at the trap sites in the light areas, and holes migrate by diffusion or drift in the presence of an external electric field to generate an internal electric field between the light and dark positions; (d) the orientation of the spontaneous polarization vector (i.e., orientation of mesogens in the FLCs) is altered by the internal electric field.

3. Asymmetric energy exchange in photorefractive materials

The phase of the refractive index grating formed by photorefractive effect is shifted from the interference fringe because the change in refractive index is induced between the bright and the dark positions of the interference fringe. In an ideal case, the phase of the refractive index grating is shifted from the interference fringe by $\pi/2$.This is a distinctive feature of the photorefractive effect. When a refractive index grating is formed via a photochemical reaction or thermal change in density, the change in refractive index occurs at the bright areas and forms a refractive index grating with the same phase as that of the interference fringe (Figure 8(a)). The induced grating diffracts the interfering laser beams; however, the apparent transmitted intensities of the laser beams do not change because beam 1 is diffracted to the direction of beam 2, and beam 2 is diffracted in the direction of beam 1. However, when the phase of the refractive index grating is shifted from that of the interference fringe (photorefractive grating), the apparent transmitted intensity of beam 1 increases and that of beam 2 decreases (Figure 8(b)). This phenomenon is known as the asymmetric energy exchange in the two-beam coupling [3]. The occurrence of the asymmetric energy exchange is the evidence for the photorefractive effect. Therefore, two-beam coupling measurement is the most straightforward way to unambiguously distinguish between the photorefractive effect and other types of grating. In LCs and low-glass-transition temperature polymers, the sign of the electro-optic coefficient is determined by the direction of the applied electric field. A change in the electric field polarity reverses the sign of the gain coefficient due to the change in sign of the electro-optic coefficient. Thus, the amplification and attenuation of beam 1 and beam 2 switches when the polarity of the applied electric field is reversed.

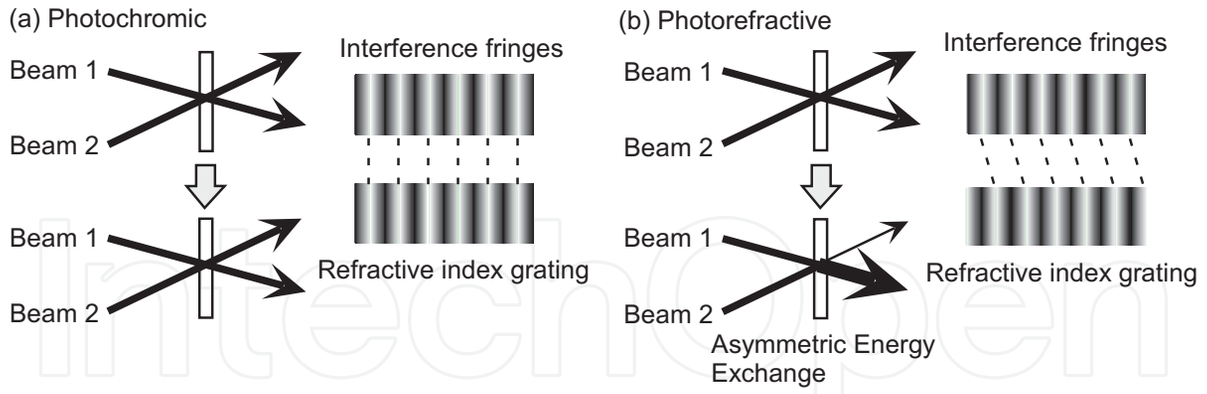

Figure 8. Schematic illustrations of (a) photochromic and (b) photorefractive gratings.

A schematic illustration of the setup used for the two-beam coupling experiment is shown in Figure 9(a). Laser beams (p-polarized) are interfered in the sample. An electric field (external electric field) is applied to the sample to increase the efficiency of charge generation in the film. The transmitted intensities of the laser beams through the sample are monitored. If a material exhibits photorefractive effect, an asymmetric energy exchange is observed. The magnitude of photorefractive effect is evaluated by the magnitude of gain coefficient, which is obtained from the two-beam coupling experiment [3]. According to the standard theory of the photorefractive effect with the limit of the ratio of beam intensities (pump/signal) >>1, the intensity of the transmitted signal beam is given by:

$$I = I_0 \exp(\Gamma l), \tag{1}$$

where I_0 is the signal beam intensity, l is the interaction length in the sample, and Γ is the gain coefficient. In order to obtain the two-beam coupling gain coefficient, the diffraction condition must be clarified whether it is in the Bragg diffraction regime or in the Raman-Nath diffraction regime. The diffraction conditions are distinguished by a parameter Q [3]:

$$Q = 2\pi\lambda L / n\Lambda^2, \tag{2}$$

where λ is the wavelength of the laser, L is the interaction path length, n is the refractive index, and Λ is the grating spacing. If the Q value is larger than 1, the condition is classified to the Bragg regime of optical diffraction in which only one order of diffraction is allowed. If Q value is smaller than 1, the condition is classified to the Raman-Nath regime of optical diffraction in which many orders of diffraction are allowed. In order to guarantee the entire Bragg diffraction regime, $Q > 10$ is often required.

The two-beam coupling gain coefficient Γ (cm^{-1}) for the Bragg diffraction condition is calculated according to the following equation [5]:

http://dx.doi.org/10.5772/60776

$$\Gamma = \frac{1}{D}\ln\left(\frac{gm}{1+m-g}\right), \tag{3}$$

where $D = L/\cos(\theta)$ is the interaction path for the signal beam (L = sample thickness, θ = propagation angle of the signal beam in the sample), g is the ratio of the signal beam intensities behind the sample with and without a pump beam, and m is the ratio of the beam intensities (pump/signal) in front of the sample.

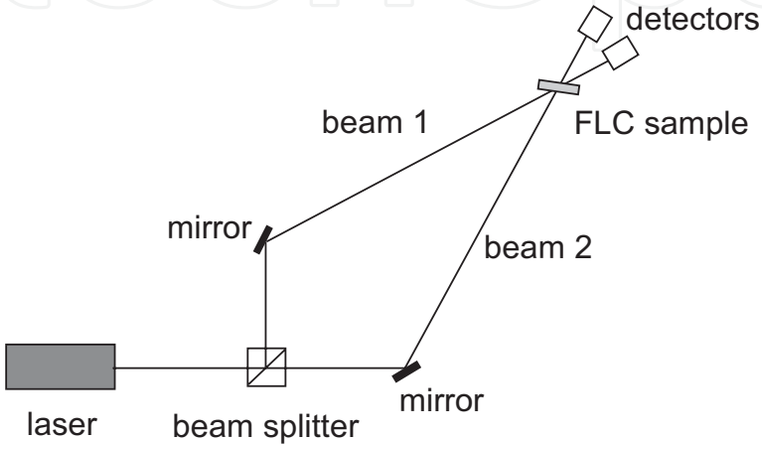

Figure 9. Schematic illustration of the experimental setup for the two-beam coupling experiment.

4. Photorefractive effect of FLCs

4.1. Two-beam coupling experiments on FLCs

Investigations into the photorefractive effect of FLCs started in the year 2000 [12, 13]; the photorefractive FLC is a mixture of FLC and photoconductive compounds. Further details of the photorefractivity in FLC materials have since been investigated by Sasaki et al. and Talarico et al. [14-19]. The structures of the photoconductive compounds used are shown in Figure 10. A commercially available FLC, SCE8 (Clariant, SmC* 60 °C SmA 80 °C N* 104 °C I, spontaneous polarization = 4.5 nC/cm^2), was used in preliminary investigations. SCE8 is a mixture of LC compounds and chiral compounds. Carbazole diphenylhydrazone (CDH) as a photoconductive compound and trinitrofluorenone (TNF) as a sensitizer were used at concentrations of 2 wt.% and 0.1 wt.%, respectively. The samples were injected into a 10 μm gap glass cell equipped with 1 cm^2 indium tin oxide electrodes and a polyimide alignment layer (Figure 11). A typical example of asymmetric energy exchange observed in the FLC (SCE8)/CDH/TNF sample under an applied DC electric field of 0.1 V/μm [17] is shown in Figure 12. The grating formation was within the Bragg diffraction regime. Interference of the laser beams in the FLC medium resulted in increased transmittance of one beam and decreased transmittance of the other. The

transmitted intensities of the two beams changed symmetrically, indicating that the phase of the refractive index grating is shifted from that of the interference fringe as shown in Figure 12.

The temperature dependence of the gain coefficient of the FLC (SCE8) doped with 2 wt.% CDH and 0.1 wt.% TNF is shown in Figure 13(a). In this sample, asymmetric energy exchange was observed only at temperatures below 46 °C. Figure 13(b) shows the temperature dependence of the spontaneous polarization of the identical sample. When the temperature was raised above 46 °C, the magnitude of the spontaneous polarization dropped to zero. Thus, the photorefractive effect of the FLC was observed only at temperatures where the sample exhibits ferroelectric phase. The reorientation associated with spontaneous polarization is induced by the internal electric field in the ferroelectric phase. The change in the direction of spontaneous polarization causes a change at the orientation of FLC molecules in the corresponding area. A maximum resolution of 0.8 μm was obtained for this sample [16].

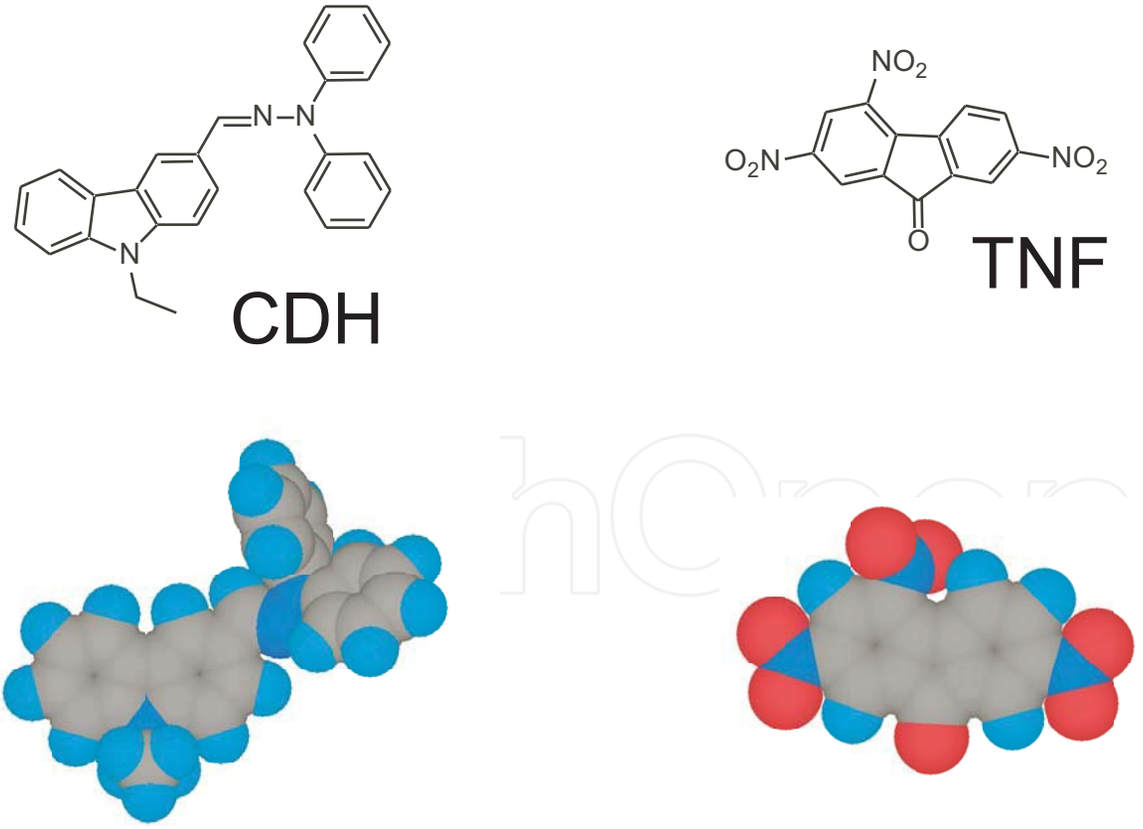

Figure 10. Structures of the photoconductive compound CDH and the sensitizer TNF.

http://dx.doi.org/10.5772/60776

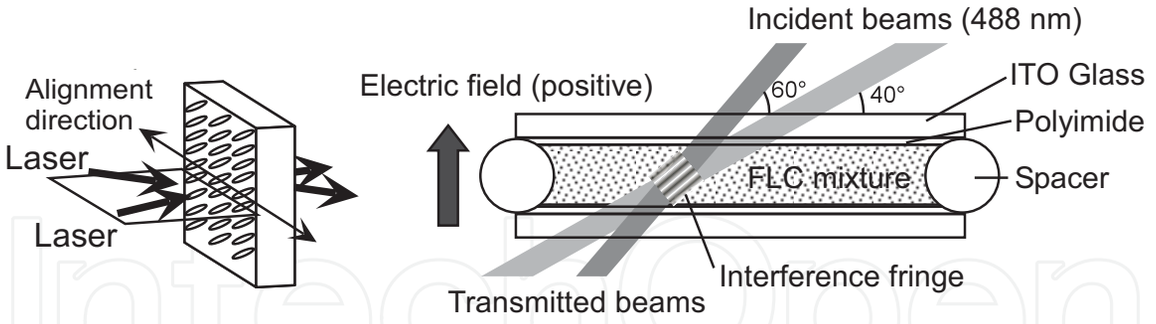

Figure 11. Laser beam incidence condition and the structure of the LC cell.

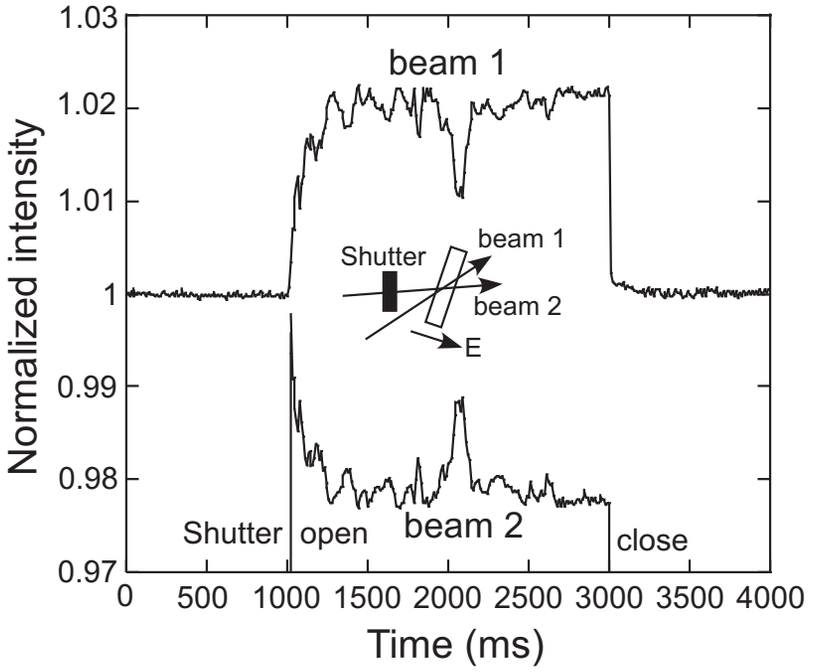

Figure 12. Typical example of asymmetric energy exchange observed in an FLC (SCE8) mixed with 2 wt.% CDH and 0.1 wt.% TNF with an electric field of +0.3 V/μm applied to the sample.

4.2. Effect of the applied electric field magnitude

The strength of the externally applied electric field is a very important factor for polymeric photorefractive materials. An external electric field is necessary to sufficiently increase the charge separation efficiency to induce a photorefractive effect; the photorefractivity of the polymer is obtained only with an electric field larger than a few volts per micrometer. The typical thickness of the polymer film for investigation of photorefractive effect is 100 μm. The strength of the voltage necessary to activate the photorefractive effect in polymer materials reaches to a few kilovolts. In contrast, the photorefractive effect in FLCs can be activated by a very weak external electric field application. The maximum gain coefficient for the FLC (SCE8)

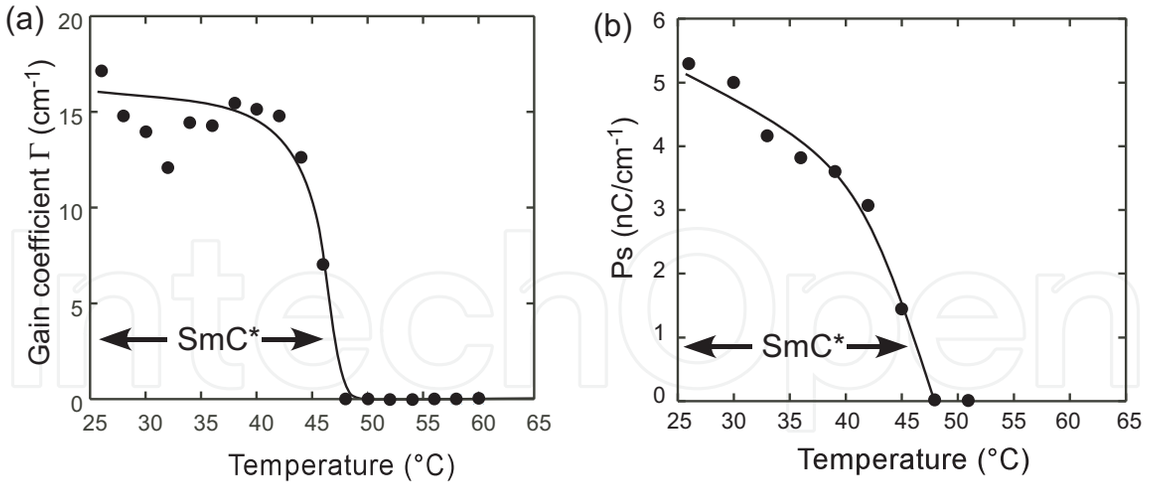

Figure 13. Temperature dependence of the (a) gain coefficient and (b) spontaneous polarization for an FLC (SCE8) mixed with 2 wt.% CDH and 0.1 wt.% TNF. For two-beam coupling experiments, an electric field of 0.1 V/μm was applied to the sample.

sample was obtained by only 0.2–0.4 V/μm electric field. The typical thickness of the photorefractive FLC sample is 10 μm; therefore, the voltage necessary to activate the photorefractive effect is only a few volts. Figure 14 shows the electric field dependence of the gain coefficient for a mixture of FLC (SCE8)/CDH/TNF. As the strength of the external electric field increased, the gain coefficient of SCE8 doped with 0.5 wt.% to 1 wt.% CDH increased. On the other hand, the gain coefficient of SCE8 doped with 2 wt.% CDH decreased when the external electric field larger than 0.4 V/μm was applied. The same tendency was also observed for another commercially available FLC; M4851/050 (Clariant, SmC* 65 °C SmA 70 °C N* 74 °C I, spontaneous polarization=14 nC/cm^2). The formation of an orientational grating is enhanced when the external electric field is increased from 0 to 0.2 V/μm due to the induced charge separation. However, when the external electric field exceeded 0.2 V/μm, a number of zigzag defects appeared in the SS-state, which caused light scattering and a decrease of the gain coefficient. The gain coefficient of FLC materials reported in the year 2003 (Figure 14) was much smaller than that of polymer materials [16].

4.3. Refractive index grating formation time

The formation of a refractive index grating involves charge separation and reorientation. The index grating formation time (response time of the photorefractive effect) is affected by these two processes, and both may act as rate-determining steps. The refractive index grating formation times for the commercially available FLCs examined (SCE8 and M4851/050) were determined on the basis of the simplest single-carrier model of photorefractivity [3, 5], wherein the gain transient is exponential. The rising signal of the diffracted beam was fitted using a single exponential function:

$$\gamma(t) - 1 = (\gamma - 1)\left[1 - \exp(-t/\tau)\right]^2, \tag{4}$$

http://dx.doi.org/10.5772/60776

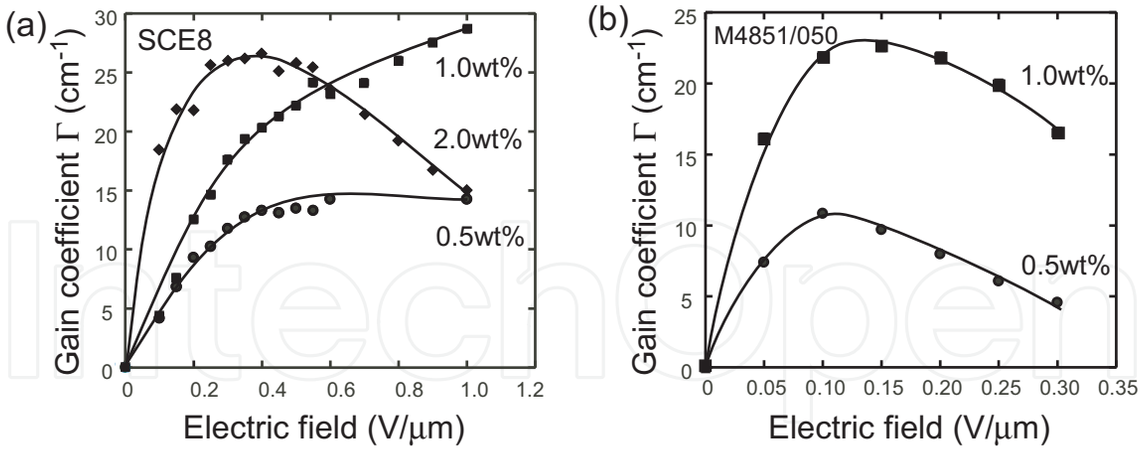

Figure 14. Electric field dependence of the gain coefficient for SCE8 and M4851/050 mixed with several concentrations of CDH and 0.1 wt.% TNF in a 10 μm gap cell measured at 30 °C.

where $\gamma(t)$ represents the transmitted beam intensity at time t, divided by the initial intensity [$\gamma(t)$ = I(t)/I0], and τ is the formation time. The grating formation time in SCE8/CDH/TNF is plotted as a function of the external electric field strength in Figure 15. The grating formation time shortened with an increase in the electric field strength because of the increased efficiency of charge generation. The formation time was shorter at higher temperatures, which corresponded to a decrease in the viscosity of the FLC with the increase in temperature. The formation time for SCE8 was 20 ms at 30 °C. The response time of FLC materials is thus faster than those of polymer materials, in which the typical response time is reported to be around 100 ms [5-8].

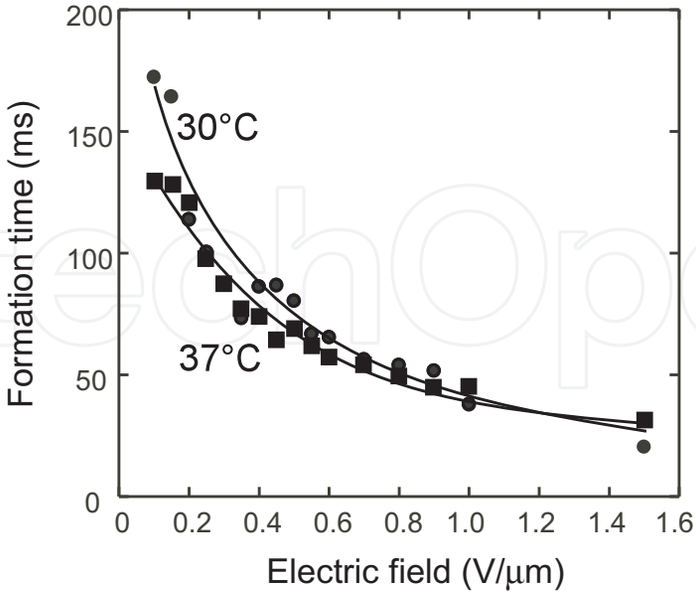

Figure 15. Electric field dependence of the index grating formation time. FLC (SCE8) mixed with 2 wt.% CDH and 0.1 wt.% TNF in a two-beam coupling experiment. ●: measured at 30 °C (T/TSmC* - SmA = 0.95); ▪: measured at 36 °C (T/TSmC* - SmA = 0.97).

5. Photorefractive effect in photorefractive FLC blends containing photoconductive chiral compounds

5.1. Photoconductive chiral dopants

FLCs are more crystalline than liquid, in comparison with nematic LCs; therefore several sophisticated techniques are required to prepare fine FLC films. Preparation of a uniformly aligned, defect-free SS-FLC using a single FLC compound is very difficult. In most cases, mixtures of LC compounds are typically used to obtain fine SS-FLC films. The composition of FLC mixture contains a base LC, which is a mixture of SmC phase forming LC compounds, and a chiral dopant. The chiral dopant introduces a helical structure into the LC phase. Utilization of an FLC as a photorefractive material requires the addition of photoconductive compounds to the FLC. However, the introduction of such non-LC compounds to the FLC often hinders the formation of a uniformly aligned SS-state. Thus, appropriate design of the photoconductive compounds is crucial. The photorefractive effect of FLC blends containing photoconductive chiral dopants has been investigated [17-19]. Terthiophene was selected as a photoconductive chromophore because it is a well-known semiconductor compound and has a rod-like structure (Figure 16), which increases the solubility into the rod-like structured LC material. The structures of the LC compounds, the electron acceptor TNF, and the photoconductive chiral compounds are shown in Figure 17. A ternary mixture of LC compounds was selected as a base LC. The mixing ratio of 8PP8, 8PP10, and 8PP6 was 1:1:2 since the 1:1:2 mixture exhibits the SmC phase over the widest temperature range. The textures of the FLC blends in 10 μm gap cells were observed using polarizing optical microscopy. The alignment of the FLC molecules is dominated not only by the properties of the FLCs but also by the affinity of FLC molecules with the alignment layer (polyimide). A homogeneous, anisotropic film can be obtained through interactions between LC molecules and the alignment layer. The FLC cell is fabricated by the precise assembly of indium tin oxide glasses coated with polyimide alignment layer into a cell of 10 μm gap determined by the diameter of the spacer bead. The appropriate preparation conditions for the fabrication of the LC cell differ from FLC to FLC. The thickness of the polyimide coating (Hitachi Chemicals LX-1400) was 20 to 30 nm and the surface of the polyimide was rubbed with a polyester velvet roll under specific conditions. Typical examples of textures observed in the 3T-2MB and 3T-2OC samples under a polarizing microscope are shown in Figures 18 and 19. On increasing the concentration of the photoconductive chiral dopant, defects appeared in the texture. The uniformly aligned state with few defects was obtained for samples with 3T-2MB concentrations lower than 8 wt.% (Figure 18). However, the 3T-2OC sample retained the uniformly aligned state with few defects for 3T-2OC concentrations less than 6 wt.% (Figure 19). The spontaneous polarization of the 3T-2MB samples was less than 1 nC/cm^2. On the other hand, the spontaneous polarization of the 3T-2OC samples was approximately 5 nC/cm^2. The smaller spontaneous polarization (and thus smaller intermolecular interactions) of the 3T-2MB sample may be advantageous for the formation of the uniformly aligned SS-state. A texture with a pattern of strips was observed in the 3T-2MB samples (Figure 18). It indicates that a complete SS-state was not formed in the 3T-2MB sample in the 10 μm gap cell and the helical structure existed. Zig-zag defect, which is the typical defect

http://dx.doi.org/10.5772/60776

in the SS-state (book shelf structure), was also observed in the texture (Figure 18). The evidence shows that the FLC mixture exhibited the SS-state in the area close to the glass surface and formed a helical structure around the center of the thickness of the 10 μm gap cell.

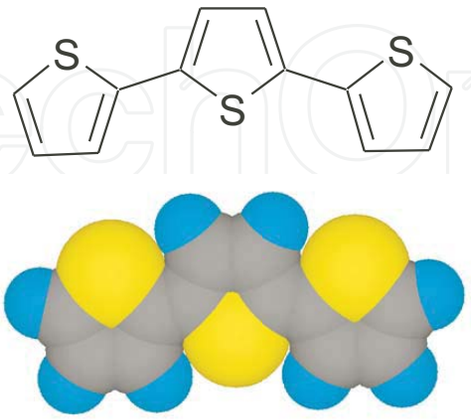

Terthiophene

Figure 16. Structure of terthiophene.

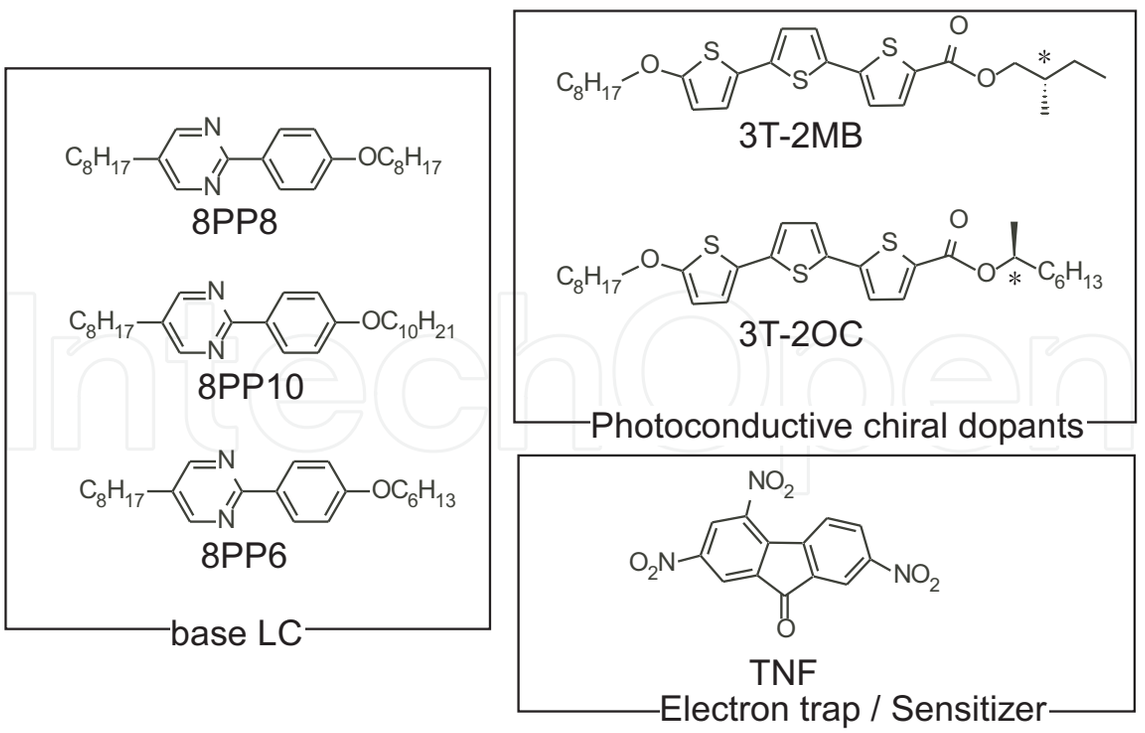

Figure 17. Structures of the smectic LCs (8PP8, 8PP10, and 8PP6), photoconductive chiral dopants (3T-2MB and 3T-2OC), and the sensitizer TNF.

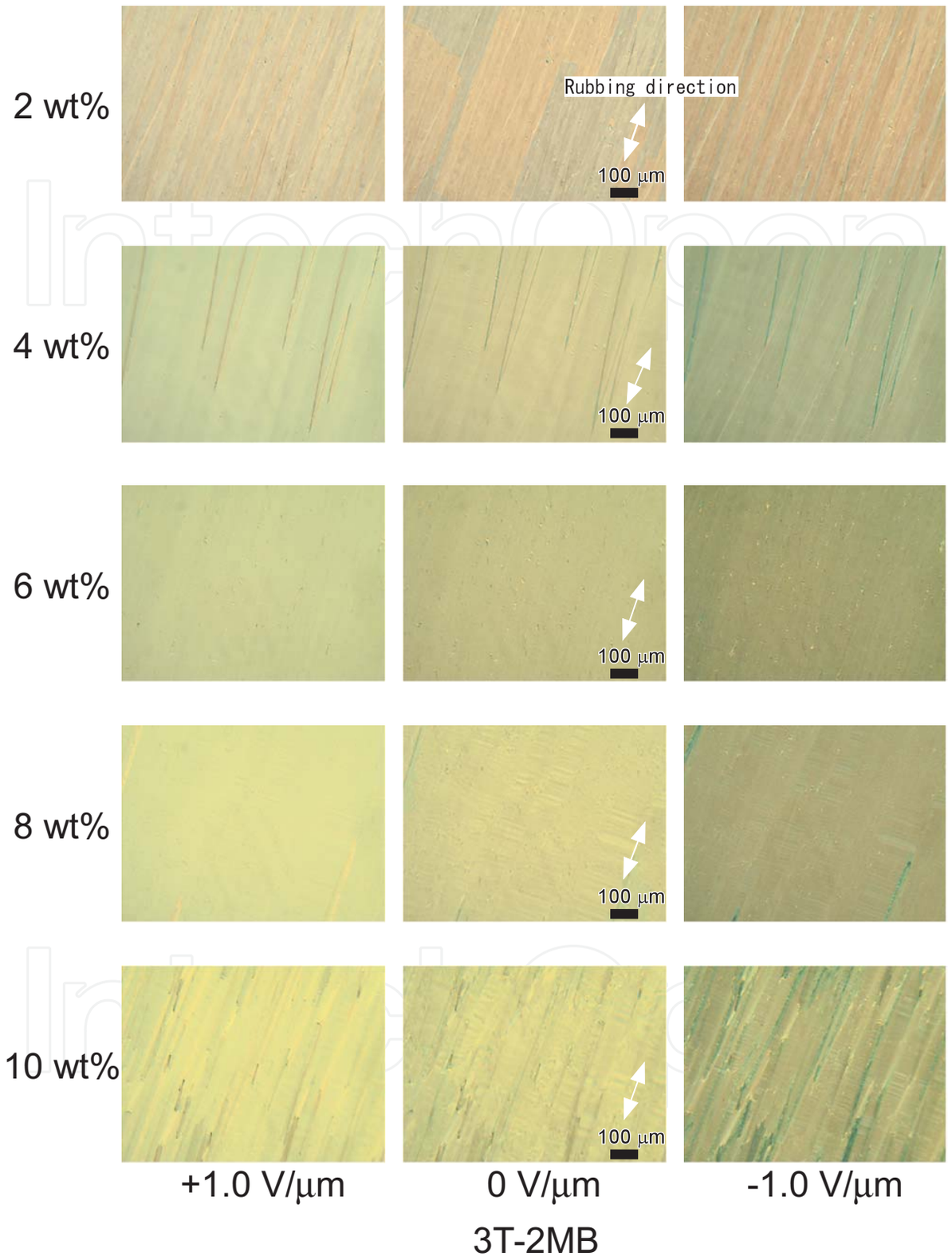

Figure 18. Textures of FLC mixtures containing 3T-2MB in a 10 μm gap LC cell observed under a polarizing microscope. The strengths of the external electric field were +1.0, 0, and 1.0 V/μm. The direction of the applied electric field is shown in Fig. 5. The 3T-2MB concentrations were in the range of 2 wt.% to 10 wt.% with the addition of 0.1 wt.% TNF.

http://dx.doi.org/10.5772/60776

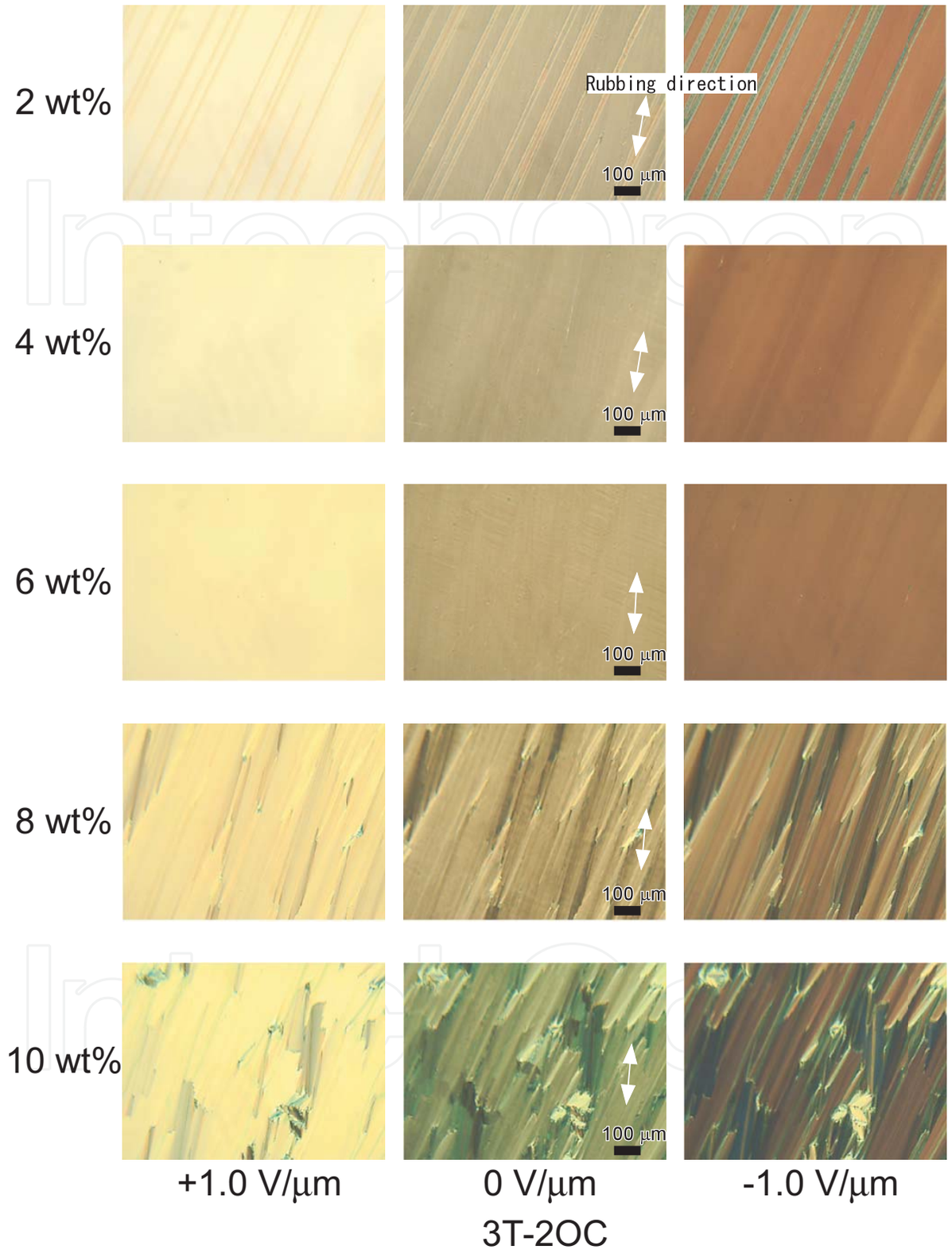

Figure 19. Textures of FLC mixtures containing 3T-2OC in a 10 μm gap LC cell observed under a polarizing microscope. The strengths of the external electric field were +1.0, 0, and 1.0 V/μm. The direction of the applied electric field is shown in Fig. 5. The 3T-2OC concentrations were in the range of 2 wt.% to 10 wt.% with the addition of 0.1 wt.% TNF.

5.2. Asymmetric energy exchange in photorefractive FLC blends

The photorefractive effect of the FLC blends was measured by two-beam coupling experiments. A typical example of the asymmetric energy exchange observed for a mixture of the base LC, 3T-2MB, and TNF at 25 °C with an applied electric field of 1 V/μm is shown in Figure 20. When the laser beams interfered in the sample, the increase in transmitted intensity of one of the beams and the decrease in the transmitted intensity of the other beam were observed. When the polarity of the applied electric field was reversed, these transmittance characteristics were also reversed. Asymmetric energy exchange was not observed when the external electric field was not applied. This indicates that the beam coupling was not caused by a thermal grating or gratings formed through photochemical mechanisms. It was found that approximately 40% of the energy of the L_2 laser beam migrated to the L_1 beam.

The gain coefficients of the samples were measured as a function of the applied electric field strength (Figure 21(a)). The gain coefficient of 1200 cm^{-1} was obtained in the 10 wt.% 3T-2MB sample with application of 1.5 V/μm. This gain coefficient is much higher than the values for FLCs reported previously [16]. The higher transparency of the LC blend was considered to contribute to the large gain coefficient. The weak external electric field strength required for the photorefractive effect in FLCs is advantageous for the photorefractive applications. The response time decreased with an increase of the electric field strength due to the increased charge separation efficiency. The shortest formation time of 0.9 ms was obtained with application of an external electric field of 1.9 V/μm (Figure 21(b)). The large gain and fast response are advantageous for the realization of optical devices such as real-time image amplifiers and accurate measurement devices.

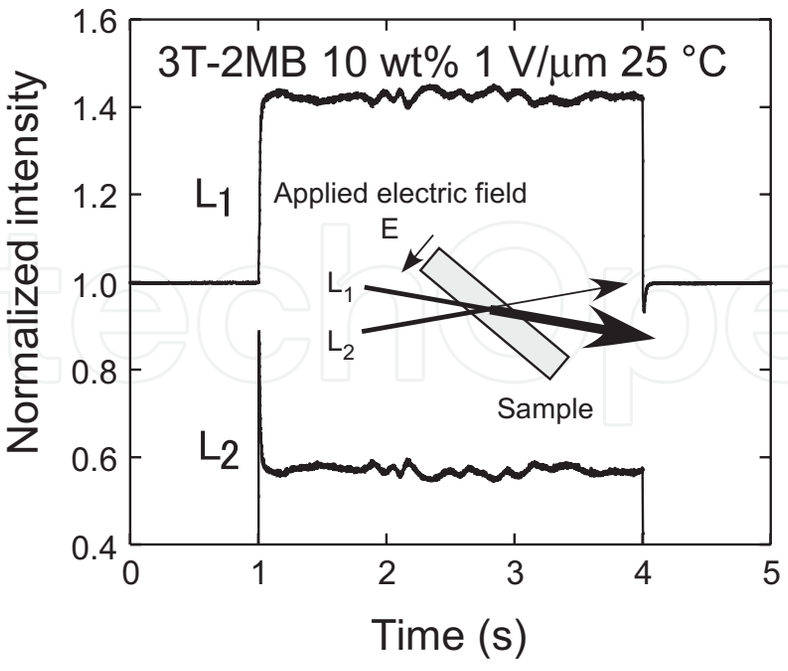

Figure 20. Typical results for two-beam coupling experiments with a ternary mixture base LC, 3T-2MB, and TNF measured at 25 °C. The pump beam was incident at 1 s and closed at 4 s.

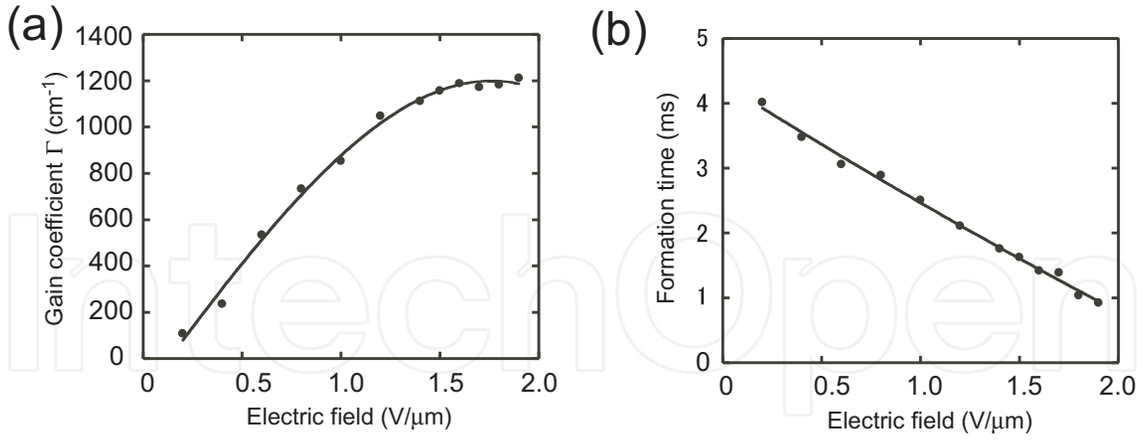

Figure 21. Electric field dependence of the (a) gain coefficients and (b) refractive index grating formation times (response time) for mixtures of the base LC, 3T-2MB (10 wt.%), and TNF (0.1 wt.%) measured at 25 °C.

5.3. Temperature dependence of the asymmetric energy exchange for photorefractive FLC blends

The temperature dependence of the gain coefficient for a photorefractive FLC blend with 3T-2MB is shown in Figure 22. Asymmetric energy exchange was observed at temperatures below the SmC*-SmA phase transition temperature. Figure 23 shows temperature dependence of the helical pitch of the 3T-2MB samples observed under polarizing microscopy. The helical pitch diverged when the temperature approached the phase transition temperature. It has been reported that the asymmetric energy exchange for an FLC sample was observed only in the temperature range where the sample exhibits spontaneous polarization [8]. Thus, asymmetric energy exchange was observed only in the temperature range where the sample exhibits ferroelectric properties (i.e., the SmC* phase).

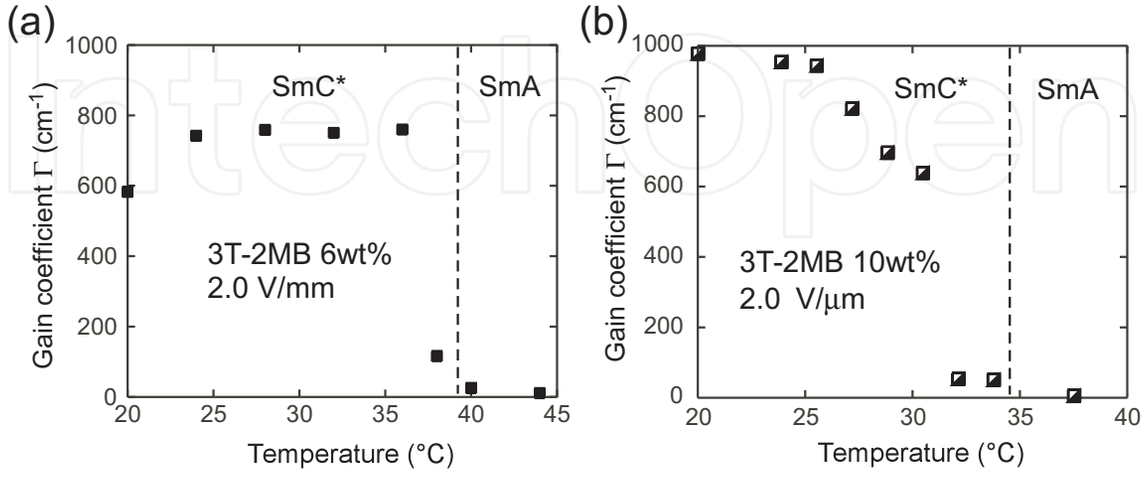

Figure 22. Temperature dependence of gain coefficients for mixtures of the base LC with 3T-2MB concentrations of (a) 6 wt.% and (b) 10 wt.%.

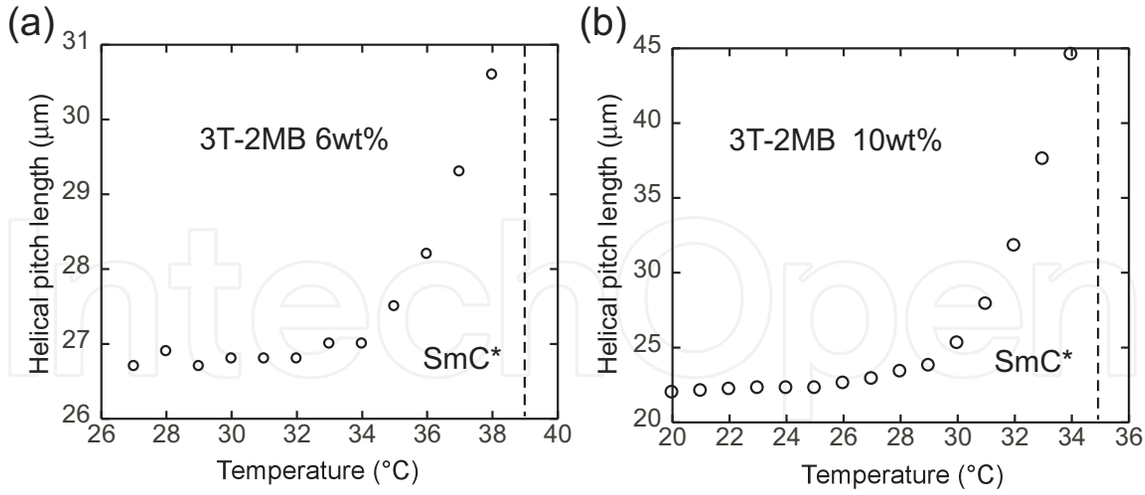

Figure 23. Temperature dependence of helical pitch lengths for mixtures of the base LC with 3T-2MB concentrations of (a) 6 wt.% and (b) 10 wt.%.

5.4. Effect of the photoconductive chiral dopant concentration

The gain coefficients of samples with various 3T-2MB and 3T-2OC concentrations are plotted as a function of the external electric field magnitude in Figure 24. The gain coefficient increased with the strength of the external electric field up to 1.6 V/μm. The decrease in the gain coefficient at high external electric field is due to the realignment of the FLC molecules being restricted because the strength of the external electric field exceeds that of the internal electric field. The gain coefficient increased with the concentration of the photoconductive chiral dopants. The increase in the concentration of charge carriers in the FLC medium and an increase in the magnitude of spontaneous polarization contributes to a larger gain coefficient. The magnitude of the gain coefficient was independent of the concentration of TNF. It shows that charges are drifted through electric conduction based on a hopping mechanism, where electron holes hop between the photoconductive chiral dopants. The molecular weight of the photoconductive chiral dopant is similar to that of the LC molecules; therefore, in a 10 wt.% doped sample, approximately 10 photoconductive molecules are dispersed in 90 LC molecules. A cube, wherein each side includes 5 LC molecules, contains 125 LC molecules. Thus, the average distance between the photoconductive chiral dopant molecules in the LC is no more than 3 LC molecules. In this case, charge transport based on a hopping mechanism may be feasible. The gain coefficient of the 10 wt.% 3T-2MB sample was 1200 cm^{-1} with an applied electric field of only 1.6 V/μm (Figure 24(a)), which is twice as high as that of the 8 wt.% 3T-2OC sample at a similar external electric field (Figure 24(b)).

The response time of the samples is plotted as a function of the external electric field magnitude in Figure 25. The response time decreased with the increase of the electric field strength due to increased charge separation efficiency. The shortest formation time of 0.93 ms was obtained for the 10 wt.% 3T-2MB sample with an applied electric field of 2.0 V/μm. It was found that the response was faster than that of the 3T-2OC samples. The gain coefficient is lower and the

http://dx.doi.org/10.5772/60776

response speed slower for the 3T-2OC sample even though the magnitude of the spontaneous polarization in the 3T-2OC samples (5 nC/cm^2) is higher than that in the 3T-2MB sample (less than 1 nC/cm^2). The transparency of the FLC film is more important for the photorefractive effect than the magnitude of spontaneous polarization.

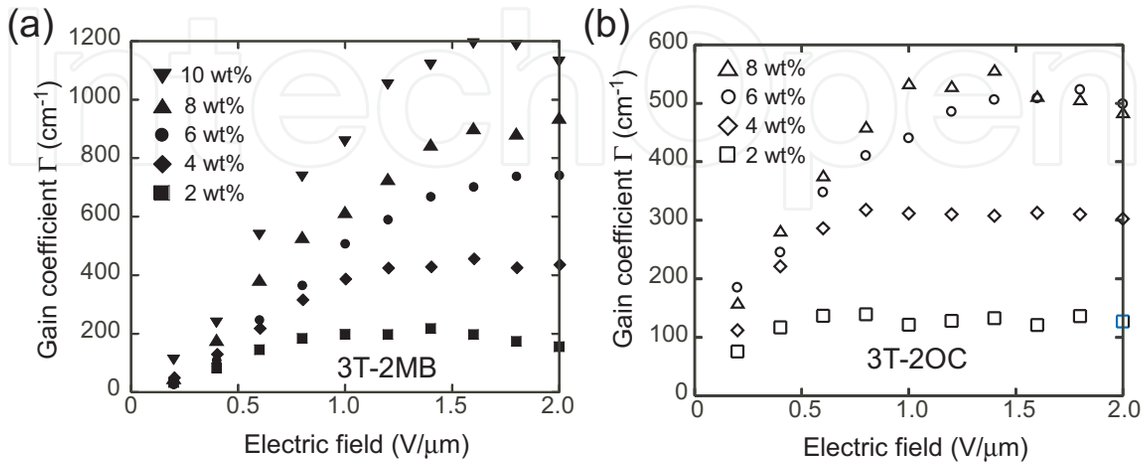

Figure 24. Electric field dependence of the gain coefficients for (a) mixtures of the base LC, 3T-2MB (2-10 wt.%), and TNF (0.1 wt.%), and (b) mixtures of the base LC, 3T-2OC (2-8 wt.%), and TNF (0.1 wt.%) measured at 25 °C.

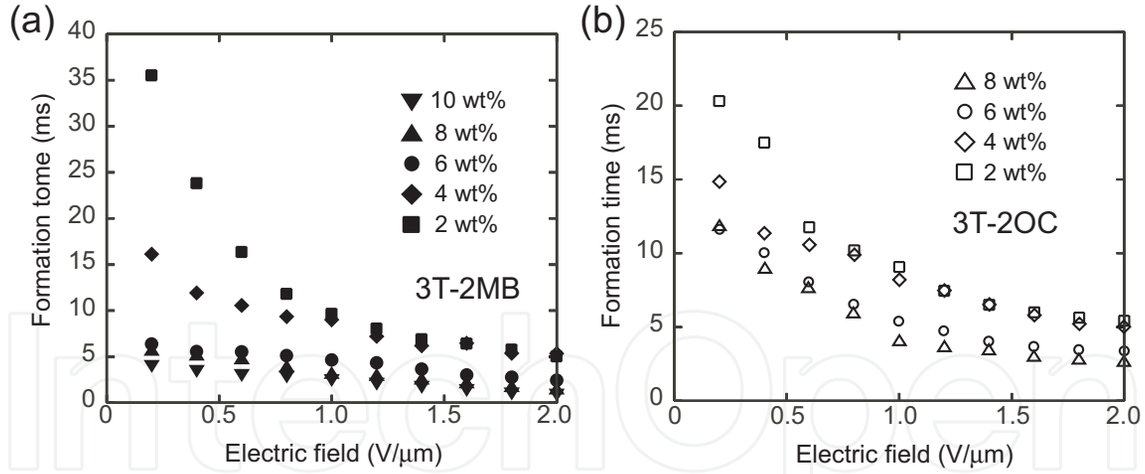

Figure 25. Refractive index grating formation times (response time) for (a) mixtures of the base LC, 3T-2MB (2-10 wt. %), and TNF (0.1 wt.%), and (b) mixtures of the base LC, 3T-2OC (2-8 wt.%), and TNF (0.1 wt.%) measured at 25 °C.

5.5. Dynamic amplification of optical images in photorefractive FLC blends

The most straightforward application of the photorefractive effect is the amplification of optical signals, which is one of the important elements of optical technologies. Light amplification based on stimulated emission and non-linear optical effects are well known. Distinct from these phenomena, the photorefractive effect enables selective amplification. The photo-

refractive effect is based on the formation of holograms in a material; therefore, it distinguishes a specific light signal from other light signals based on the difference in wavelength, polarization, and phase. Optical image amplification was demonstrated (Figure 26), where a computer-generated image was displayed on a spatial light modulator (SLM) and irradiated with a 473 nm diode-pumped solid-state laser beam [18]. A signal laser beam carrying a 2D image was transmitted through the FLC sample. The image was monitored with a charge-coupled device (CCD) camera. A pump beam (a beam divided from the signal beam before SLM) was interfered with the signal beam. The amplification of the signal beam transmitted through the FLC was observed. The intensities of the optical signal beam with and without the pump beam are shown in Figure 27. The intensity of the signal beam was amplified six-fold to the value without the pump beam.

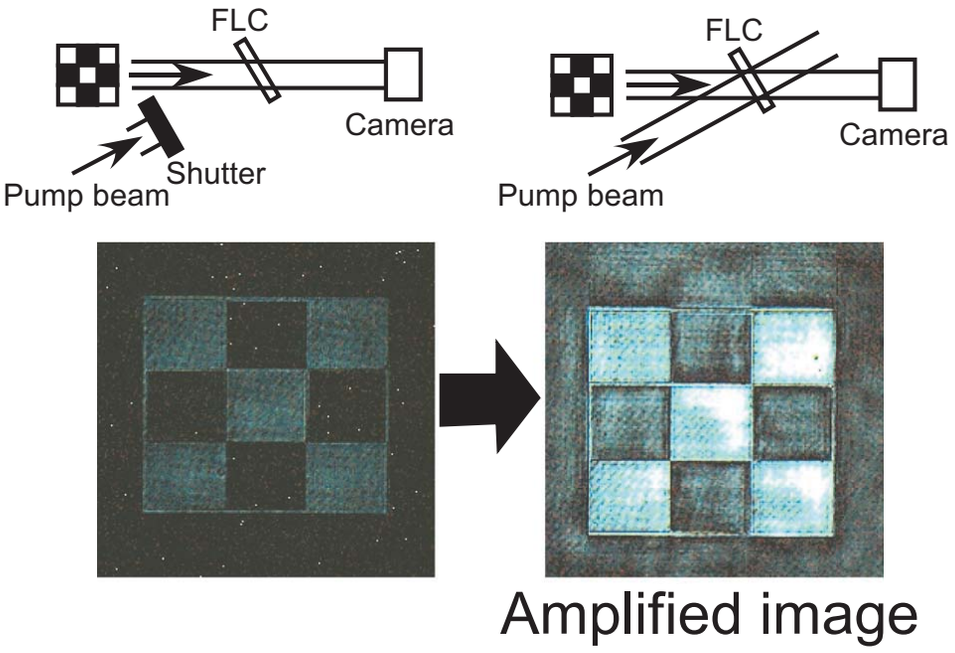

Figure 26. Optical image amplification experiment. A computer-generated image was displayed on the SLM. The SLM modulated the object beam (473 nm), which was irradiated on the FLC sample and interfered with the pump beam. The image transmitted through the FLC sample (10 wt.% 3T-2MB) was monitored with a CCD camera.

Dynamic amplification of moving optical signal was demonstrated using a photorefractive FLC blend [18]. A rotating image was displayed on the SLM with the frame rate at 30 fps. A 473 nm beam was irradiated on the SLM and the reflected beam was incident on the FLC sample. A pump beam was then interfered with the beam from the SLM in the FLC sample. The laser beam containing the moving animation image was amplified by the incident pump beam (Figure 28). This result shows that the response of the photorefractive FLC was sufficiently fast to amplify the moving optical image. If a typical photorefractive polymer with a response time of ca. 100 ms was used in place of the FLC sample, then the moving image would not be amplified. In that case, although a still image could be amplified, the intensity of the video-rate moving image would not be amplified.

http://dx.doi.org/10.5772/60776

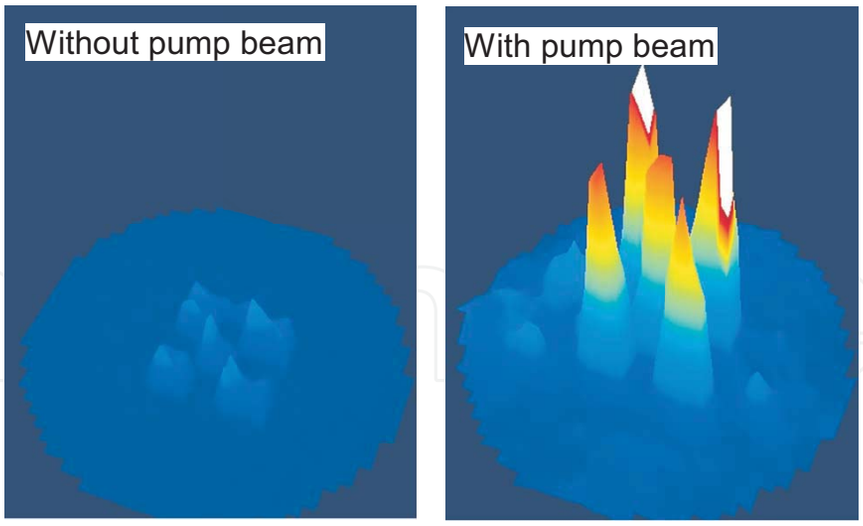

Figure 27. Signal beam intensities with and without the pump beam.

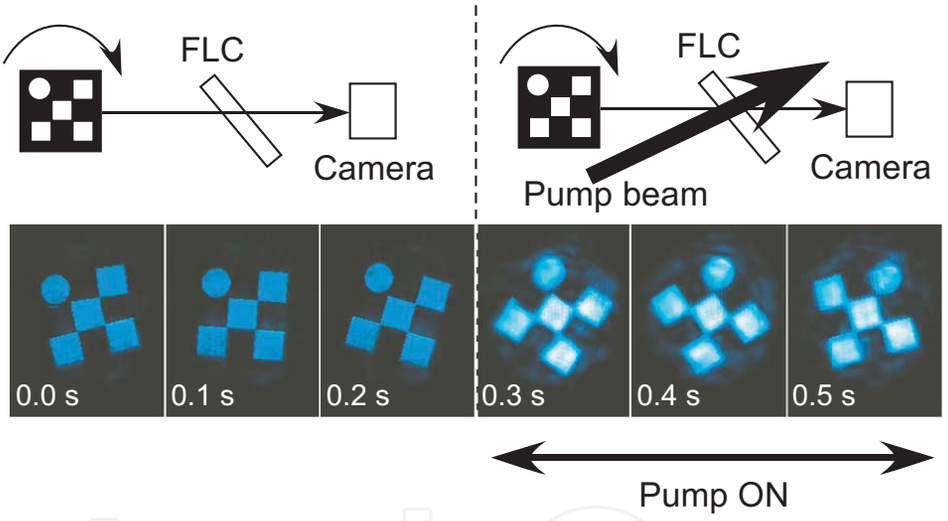

Figure 28. Optical image amplification experiment. A computer-generated animation was displayed on the SLM. The SLM modulated the object beam (473 nm), which was irradiated on the FLC sample, and interfered with the reference beam. The image transmitted through the FLC sample (10 wt.% 3T-2MB) was monitored with a CCD camera.

5.6. Dynamic holograms formed in FLC blends

Dynamic hologram formation was demonstrated in an FLC blend [19]. A moving image was displayed on an SLM and a laser beam was irradiated onto the SLM. The reflected beam was incident on the FLC sample and a reference beam was then interfered with the beam within the FLC sample. The interference condition was set to a Raman–Nath diffraction regime. The multiple scattering was observed in this condition. A red beam from a He–Ne laser (633 nm) was incident on the FLC sample and the diffraction was observed. A moving image was observed in the diffracted beam (Figure 29). No image retention was observed, which indicates

that the hologram image (refractive index grating) formed in the FLC was rewritten with sufficient speed to project a smooth reproduction of the holographic movie. This result shows that a hologram image was formed at the interference area in the FLC material and that contributes to the optical image amplification.

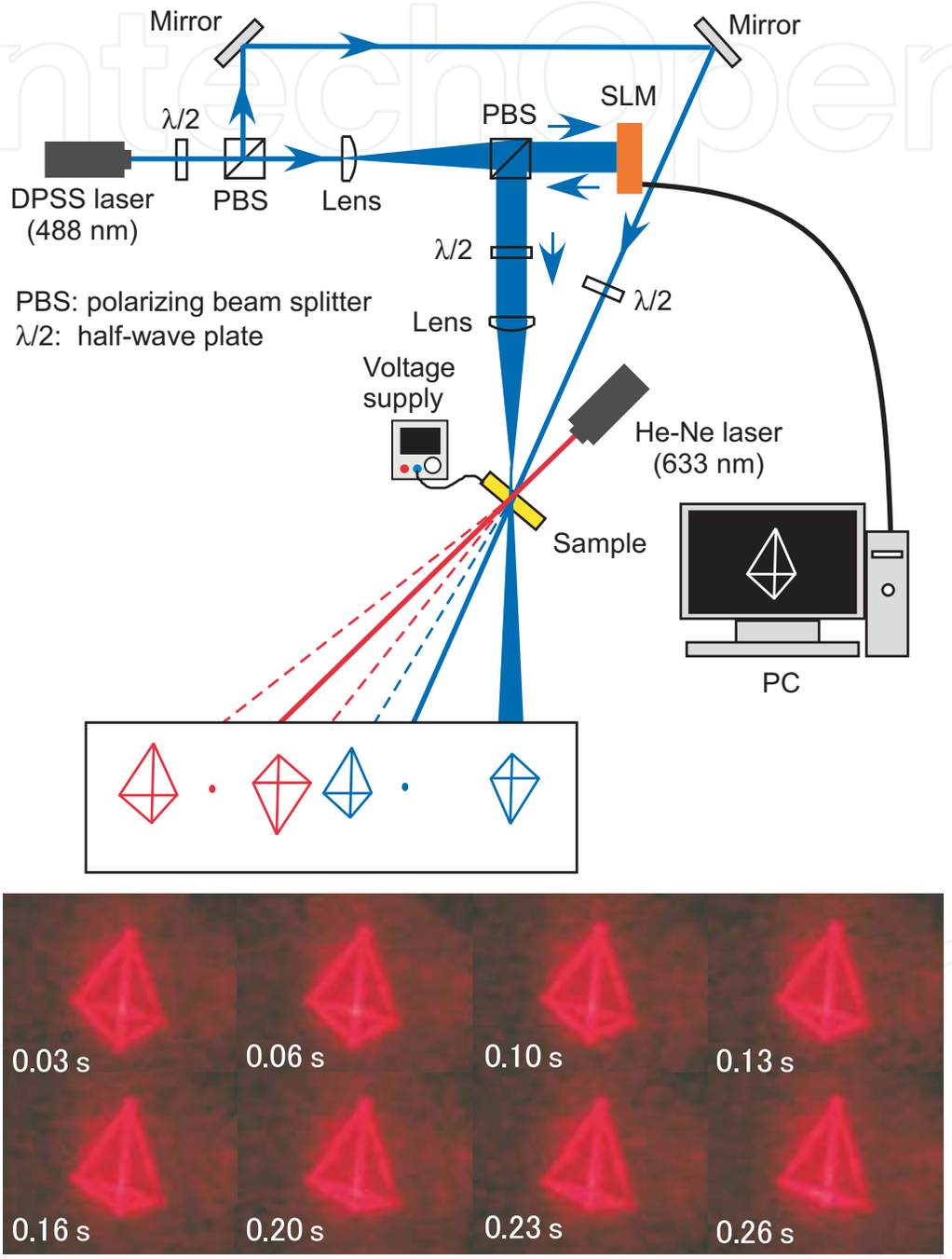

Figure 29. Dynamic hologram formation experiment on an FLC sample. A computer-generated animation was displayed on the SLM. The SLM modulated the object beam (488 nm), which was irradiated on the FLC sample and allowed to interfere with the reference beam. The readout beam (633 nm) was irradiated on the FLC and diffraction was observed.

http://dx.doi.org/10.5772/60776

6. Conclusions

Real-time dynamic amplification of optical image signals was demonstrated in photorefractive FLC blends. The response time was of sub-millisecond order and was dominated by the formation of an internal electric field. The photorefractive effect of FLCs was significantly dominated by the properties of the FLCs. Aside from spontaneous polarization, viscosity, and the phase transition temperature, the homogeneity of the SS-state was found to be a major factor. The gain coefficient and the response time were also significantly dominated by the homogeneity of the SS-state. Therefore, a highly homogeneous SS-state is necessary to create a photorefractive device. A gain coefficient higher than 1200 cm^{-1} and a response time shorter than 1 ms were obtained with application of only 1.5 V/μm in a photorefractive FLC blend. This response time is sufficiently short for real-time dynamic holograms. FLC mixtures containing photoconductive chiral dopants exhibited high gain coefficients and fast responses, which confirms their usefulness in photorefractive device applications.

Acknowledgements

The authors would like to thank the Japan Science and Technology Agency S-innovation and the Canon Foundation for support.

Author details

Takeo Sasaki

Address all correspondence to: Sasaki@rs.kagu.tus.ac.jp

Tokyo University of Science,Tokyo, Japan

References

[1] Skarp, K.; Handschy, M.A. *Mol Cryst Liq Cryst.* 1988, *165*, 439-569.

[2] Oswald, P.; Pieranski, P. *Smectic and Columnar Liquid Crystals*; Taylor & Francis: New York, 2006.

[3] Solymar, L.; Webb, J.D.; Grunnet-Jepsen, A. *The Physics and Applications of Photorefractive Materials*; Oxford: New York, 1996.

[4] Goonesekera, A.; Wright, D.; Merner, W.E. *Appl Phys Lett.* 2000, *76*, 3358-3361.

[5] Moerner, W.E.; Silence, S.M. *Chem Rev*. 1994, *94*, 127-155.

[6] Kippelen, B.; Peyghambarian, N. *Advances in Polymer Science, Polymers for Photonics Applications II*; Springer: 2002, 87-156.

[7] Ostroverkhova, O.; Moerner, W.E. *Chem Rev.* 2004, *104*, 3267-3314.

[8] Sasaki, T. *Polym J.* 2005, *37*, 797-812.

[9] Tay, S.; Blanche, P.A.; Voorakaranam, R.; et al. *Nature*, 2008, *451*, 694-698.

[10] Blanche, P.A.; Bablumian, A.; Voorakaranam, R.et al. *Nature*, 2010, *468*, 80-83.

[11] Khoo, I.C. *Liquid Crystal Photorefractive Optics.* In: Yu, F.T.S (ed) *Photorefractive Optics*; Academic Press: 2000.

[12] Wiederrecht, G.P., Yoon, B.A., Wasielewski, M.R. *Adv Mater.* 2000, *12*, 1533-1536.

[13] Sasaki, T.; Kino, Y.; Shibata, M.; et al. *Appl Phys Lett.* 2001, *78*, 4112-4114.

[14] Talarico, M.; Goelemme, A. *Nature Mater*. 2006, *5*, 185-188.

[15] Meyer, R.B. *Mol Cryst Liq Cryst.* 1977, *40*, 33-48.

[16] Sasaki, T.; Naka, Y. *Opt Rev.* 2014, *21*, 99-109.

[17] Sasaki, T.; Miyazaki,D.; Akaike, K.; Ikegami, M.; Naka, Y. *J Mater Chem*. 2011, *21*, 8678-8686.

[18] Sasaki, T.; Kajikawa, S.; Naka, T. *Faraday Discuss.* 2014, *174*, 203-218.

[19] Sasaki, T.; Ikegami, M.; Abe, T.; et al. Appl Phys Lett. 2013, 102, 063306 (1-3).